Colloids and Surfaces A: Physicochem. Eng. Aspects 422 (2013) 199–205

Contents lists available at SciVerse ScienceDirect

Colloids and Surfaces A: Physicochemical and Engineering Aspects

journal homepage: www.elsevier.com/locate/colsurfa

ZnO hollow microspheres with exposed porous nanosheets surface: Structurally enhanced adsorption towards heavy metal ions

Xianbiao Wang[a,b,*], Weiping Cai[a,*], Shengwen Liu[a], Guozhong Wang[a], Zhikun Wu[a], Huijun Zhao[c,*]

[a] Key Laboratory of Materials Physics, Anhui Key Laboratory of Nanomaterials and Nanotechnology, Institute of Solid State Physics, Chinese Academy of Sciences, Hefei 230031, PR China
[b] Anhui Key Laboratory of Advanced Building Materials, School of Materials and Chemical Engineering, Anhui University of Architecture, Hefei 230601, PR China
[c] Centre for Clean Environment and Energy, Gold Coast Campus, Griffith University, Queensland 4222, Australia

HIGHLIGHTS

- The standing and cross-linked porous nanoplate-built ZnO hollow microspheres are fabricated.
- Such microspheres exhibit significantly structurally enhanced adsorption to heavy metal cations.
- This material show much higher adsorption capacity than activated carbon reported previously.
- The adsorption performance of this material depends on the electronegativity of the heavy metals.

GRAPHICAL ABSTRACT

The micro/nanostructured ZnO hollow spheres built of porous nanosheets were fabricated through hydrothermal treatment. Such hollow spheres with exposed porous nanosheets surface exhibit significantly structurally enhanced adsorption performance for heavy metal ions compared with the commercial ZnO nanopowders. (a) ZnO hollow spheres; (b) the adsorption isotherms of Cu(II) on ZnO hollow spheres compared with that of commercial ZnO nanopowders.

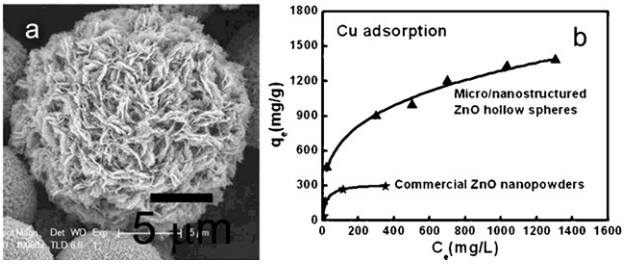

ARTICLE INFO

Article history:
Received 24 August 2012
Received in revised form 11 January 2013
Accepted 22 January 2013
Available online 29 January 2013

Keywords:
Standing porous nanosheet-built ZnO hollow micro-spheres
Structurally enhanced adsorption
Electronegativity dependence

ABSTRACT

The micro/nanostructured materials can be used for the high efficient adsorbents owing to their high specific surface area, high surface activity and high stability against aggregation. In this paper, standing porous nanosheet-built ZnO hollow microspheres are produced through a modified hydrothermal route. Such ZnO hollow microspheres with exposed porous nanosheets surface exhibit significantly structurally enhanced adsorption performance for heavy metal cations [Cu(II), Pb(II), Cd(II), and Ni(II), etc.], compared with the commercial ZnO nanopowders, and show much higher adsorption capacities than the surface functionalized activated carbon reported previously. The adsorption isotherms can be described by Langmuir model or Freundlich model, depending on the electronegativity of the heavy metals. This ZnO hollow microspheres with exposed porous nanosheets surface can be used as adsorbent for efficient removal of heavy metal ions from the contaminated water with weak acidity or alkalescence, and easily separated from solution. This study also deepens understanding adsorption behavior of micro/nanostructured ZnO to heavy metal cations.

1. Introduction

The water pollution caused by heavy metal ions has been much concerned due to their high toxicity [1–3]. There are a lot of techniques developed for its remediation [4–8]. Recently removal of heavy metal ions by adsorption has been an effective method [6–8].

* Corresponding author at: Key Laboratory of Materials Physics, Anhui Key Laboratory of Nanomaterials and Nanotechnology, Institute of Solid State Physics, Chinese Academy of Sciences, Hefei 230031, PR China. Tel.: +86 551 65592747.
E-mail addresses: xbwang@issp.ac.cn (X. Wang), wpcai@issp.ac.cn (W. Cai), h.zhao@griffith.edu.au (H. Zhao).

0927-7757/$ – see front matter © 2013 Elsevier B.V. All rights reserved.
http://dx.doi.org/10.1016/j.colsurfa.2013.01.031

Obviously, the absorbents with high specific surface area, high surface activity and high structural stability are highly expected. The nanomaterials could be good adsorbent owing to their high specific surface area and surface activity. However, they are very easily aggregated which leads to significant decrease of the active surface area. The micro/nanostructured materials could solve this problem owing to their unique structure of microsized objects with nanostructures [9], which can effectively resist aggregation. Therefore, the micro/nanostructured mateirals can be applied for high efficient removal of heavy metal ions.

Many micro/nanostructured materials have been used as adsorbents for removal of heavy metal ions and organic contaminants in wastewater. For instance, Chrysanthemum-like α-FeOOH was used for removal of heavy metal ion with high adsorption efficiency and capacity [10]. Micro/nanostructured CeO_2 [11,12]and Y_2O_3 [13] were adopted for adsorption of Cr(VI) species. In our previous work, hierarchical porous carbon was prepared and applied in contaminants removal with high efficiency [14].

It is well known that ZnO is a promising candidate for photocatalyst [15,16], sensor [17], solar cell [18], and so on [19]. There have been extensive reports in these fields. Also, ZnO is an environmental friendly material and its surface has many functional groups, such as hydroxyl groups, which can be active sites for adsorption [20,21]. ZnO with micro/nanostructure could thus be a good candidate as adsorbent for wastewater treatment. However, the report on micro/nanostuctured ZnO as adsorbent for environmental remediation is very limited, to our best knowledge.

Recently, we have reported micro/nanostructured ZnO porous nanoplates with high specific surface area, which showed the excellent adsorption performance to Cu(II) ions in aqueous solution and demonstrated the validity of the porous ZnO nanoplates as the promising adsorbent for contaminant-removal [22]. However, these porous nanoplates were easy to stack together or overlap, due to the planar geometry, and hence decreased the surface area exposed to the solution. The structurally enhanced adsorption performance of the micro/nanostructured material was only partially exhibited. Obviously, if we assemble these porous nanoplates into a micro/nanostructure and all the porous nanoplates are vertically standing and cross-linked, stacking or pileup of the nanoplates will not take place, or the surface area within the porous nanoplates will be sufficiently exposed to the solution. The structurally enhanced adsorption performance would thus be sufficiently exhibited. This has been confirmed in this work.

In this article, ZnO hollow microspheres with exposed porous nanosheets surface are obtained based on a modified hydrothermal route, with citrate as structural director. We have demonstrated that such material sufficiently exhibits structurally enhanced adsorption performance for heavy metal cations, compared with the porous nanoplates or commercial ZnO nanopowders. The adsorption isotherms can be described by Langmuir model or Freundlich model, depending on the electronegativity of the heavy metals. This porous nanosheet-built micro/nanostructured material can be used as an efficient adsorbent for removal of heavy metal ions [Cu(II), Pb(II), Cd(II) and Ni(II) etc.] from the contaminated water with weak acidity or alkalescence, and easily separated from solution. This study also deepens understanding adsorption behavior to metal cations.

2. Experimental

2.1. Preparation of adsorbent

The detailed preparation of the ZnO hollow microspheres with exposed porous nanosheets surface is previously reported [23]. Typically, 3 mmol zinc acetate dihydrate [$Zn(CH_3COO)_2{\cdot}2H_2O$] and 9 mmol urea [$(NH_2)_2CO$] were first dissolved in 40 ml distilled water, and 0.2 mmol trisodium citrate dihydrate ($C_6H_5Na_3O_7{\cdot}2H_2O$) was then dissolved in 10 mL distilled water. Subsequently both solutions were mixed and stirred for 30 min. The mixed solution was then transferred into a 65 mL Teflon-lined autoclave and undergone thermal treatment at 160 °C for 12 h. After reaction and cooling to the room temperature, the white products were obtained after washed with distilled water and ethanol for several times. Finally, the products were annealed at 400 °C for 2 h.

2.2. Characterization

Morphology and microstructure were examined by X-ray diffraction (XRD), field emission scanning electron microscope (FESEM, Sirion 200 FEG) and the transmission electron microscope (TEM, JEOL-2010), respectively. Nitrogen adsorption isotherms were measured at 77 K on a Micrometrics ASAP 2020 equipment. X-ray photoelectron spectroscopic (XPS) spectra were obtained with Al Kα X-ray source ($h\nu$ = 1486.6 eV) operated with pass energy of 20 eV on a Thermo ESCALAB 250 analyzer. Diffuse reflectance infrared spectroscopy (DRIFTS) was conducted on an Thermo Nicolet NEXUS FT-IR spectrometer at 298 K. The resolution was 4 cm^{-1} and KBr was used as background.

2.3. Adsorption measurements

All the adsorption experiments were carried out at 25 °C in the dark. $CuCl_2{\cdot}2H_2O$, $Cd(NO_3)_2{\cdot}4H_2O$ and $Pb(NO_3)_2$ were, respectively, used as the sources of Cu(II), Cd (II) and Pb(II) ions, which were dissolved in distilled water to obtain solutions with different concentrations. Then, a certain amount of prepared products [5 mg for adsorption of Cu(II), 10 mg for adsorption of Cd(II) and Pb(II)] was added into 10 mL solution with different initial concentrations under stirring and kept for 10 h to establish adsorption equilibrium. The initial pH value was adjusted to 4–6 for Cu(II) solution, and 6 for Cd(II) and Pb(II) solutions by dropping NaOH (0.1 M) or HNO_3 (0.1 M) solution. The concentrations of metal ions in the solution were monitored by inductively coupled plasma (ICP, IRIS Intrepid II ICP-OES). Adsorption isotherms were obtained by varying the initial concentrations of heavy metal ions. The corresponding experiments were also performed for the commercial ZnO nanopowders (5 m^2/g, Shanghai Chemical Reagent Co.) for comparison.

3. Results and discussion

3.1. Characterization of sample

After hydrothermal reaction at 160 °C for 12 h, the products were obtained and characterized. The XRD has revealed that the products are monoclinic hydrozincite $Zn_5(OH)_6$ $(CO_3)_2$ (or ZnHC for short), as previously reported [23]. The subsequent annealing at 400 °C for 2 h leads to decomposition of the ZnHC into hexagonal wurtzite ZnO with lattice parameters of a = 3.249 Å. This is in good agreement with the previous reports [22–25]. In addition, it should be mentioned that the yield of our product is estimated to be more than 70% and easy to realize mass production, as mentioned in our previous work [23].

FESEM observation shows that the annealed products consist of rough microspheres with size 5–20 μm which centered around 12 μm, as illustrated in Fig. 1a. Careful examination has demonstrated that the spherical particles are built of cross-linked and nearly vertically standing porous nanoplates or nanosheets (Fig. 1b). The uniformly distributed pores should originate from decomposition of ZnHC during annealing [22,23].By crushing the

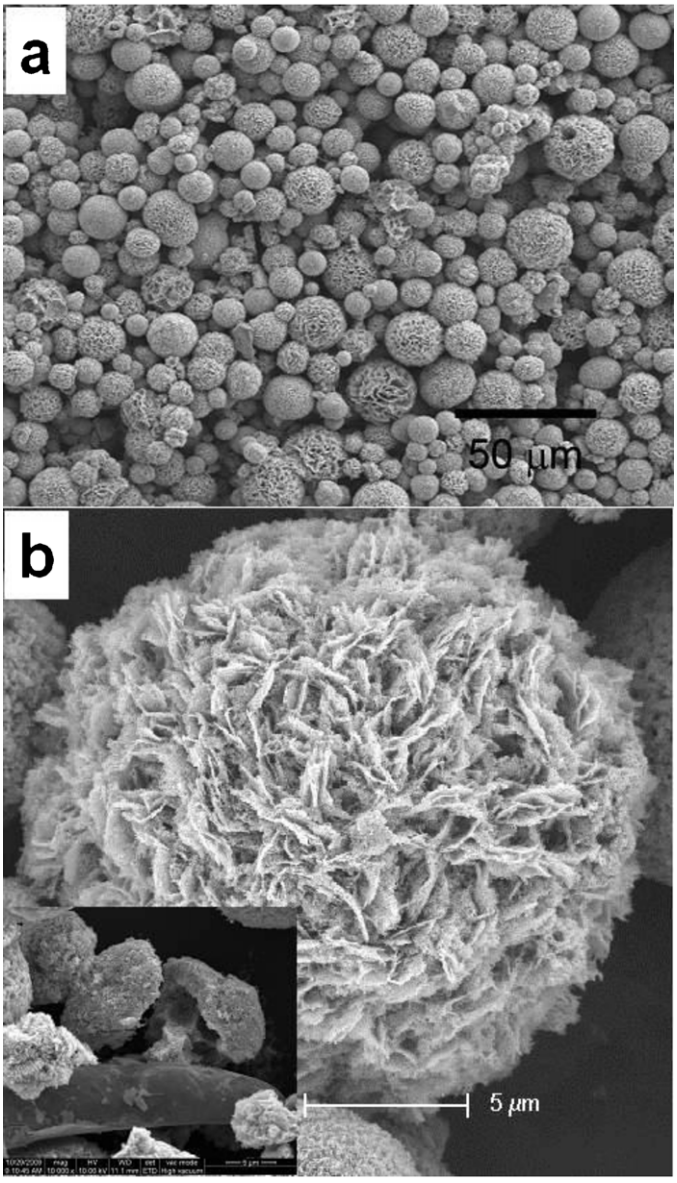

Fig. 1. FESEM images of the product after annealing. (a) Low magnification. (b) High magnification for a single sphere. The inset: a broken sphere.

spheres, the hollow structure with ~5 μm in hollow size is shown (the inset of Fig. 1b).

Further, high resolution TEM examination shows that the nanosheet is of single crystalline structure, as shown in Fig. 2. The fringes with the spacing of 0.26 nm corresponds to (0 0 0 2) plane of ZnO. The exposed surface of porous ZnO nanosheets is the non-polar (1 0 $\bar{1}$ 0) [or (1 0 0)] plane [23]. In addition, the pores within the nanoplates are around 10–15 nm in size, which can be clearly seen in Fig. 2.

Further, the isothermal nitrogen sorption measurement has indicated that it follows the typical type II sorption [23,26]. The specific surface area is thus calculated to be about 46 m^2/g according to Brunauer–Emmett–Teller (BET) equation [23,27]. Therefore, the ZnO hollow spheres could be used as high efficient adsorbent in wastewater treatment. The formation of such structured ZnO has been deep studied and reported [23]. Herein, we focused on its structurally enhanced adsorption performance for heavy metal cations.

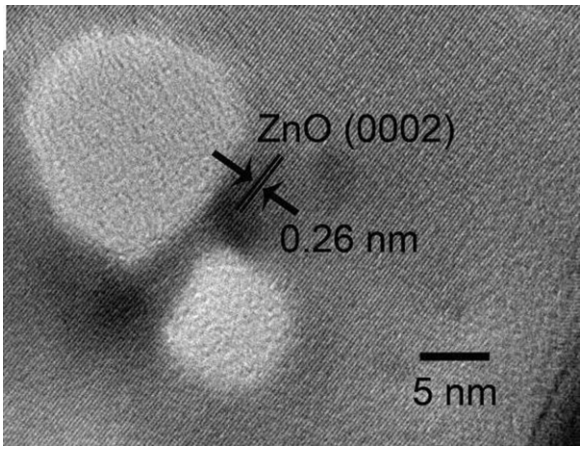

Fig. 2. High resolution TEM image for the local planar area of a single nanoplate.

3.2. Adsorption performance for heavy metal ions

It is well known that superfluous heavy metal ions in water are harmful to the health of human. Such pollutants can be removed by nano-adsorbents (carbon nanotube, carbon aerogel, etc.) [28,29]. However, these adsorbents usually suspend in the aqueous solution and are difficult to be separated, leading to the secondary pollution. Comparatively, the micro/nanostructured materials have advantages over nanopowders as adsorbents, owing to their high stability against aggregation and easy separation from solution [11]. It has been shown that the ZnO hollow microspheres with exposed porous nanosheets surface presented high efficient heavy metal-removal performance from wastewater. Here we take Cu(II), Pb(II) and Cd(II) as the adsorbates to demonstrate their adsorption capacity and behaviours on this porous ZnO hollow spheres.

3.2.1. High efficient adsorption for Cu(II) ions

The adsorption isotherm of Cu(II) ions on the ZnO hollow microspheres with exposed porous nanosheets surface is shown on curve 1 of Fig. 3a, which has been presented in supplementary material of our previous paper [23]. The adsorption capacity of Cu(II) ions increased with the concentration of Cu(II) ion in the solution. The adsorption amount is higher than 1400 mg Cu in each gram of the porous ZnO, which is much higher than that (~54 mg/g) of the surface functionalized activated carbon reported previously [30]. Importantly, no saturated adsorption was found even when the initial concentration of Cu(II) in the solution is higher than 2000 mg/L. The adsorption capacity is close to that of the previously reported porous ZnO nanoplates with much higher specific surface area (147 m^2/g) (curve 3 in Fig. 3a) [22]. It means that the ZnO hollow microspheres with exposed porous nanosheets surface exhibit much higher adsorption efficiency than the pure porous nanoplates, since it can keep high exposed active surface area during use due to its special geometry. Correspondingly, for the commercial ZnO nanopowders, the adsorption is much lower and saturated when the concentration of Cu(II) ions in the solution is up to 300 mg/L (curve 2 in Fig. 3a), as we previously mentioned [22].

Further, the adsorption isotherm on this porous ZnO hollow spheres (curve 1 in Fig. 3a) well follows Freundlich model [31], which describes adsorption on heterogeneous surface, or

$$q_e = K_F \times C_e^{1/n} \quad (1)$$

where K_F ($mg^{1-1/n}\,L^{1/n}\,g^{-1}$) and n are the parameters reflecting the adsorption capacity and the adsorption intensity, respectively. Fig. 3b gives the corresponding plots of $\lg q_e \sim \lg C_e$, exhibiting good linear relationship. The parameters K_F and n are fitted to be 177 and

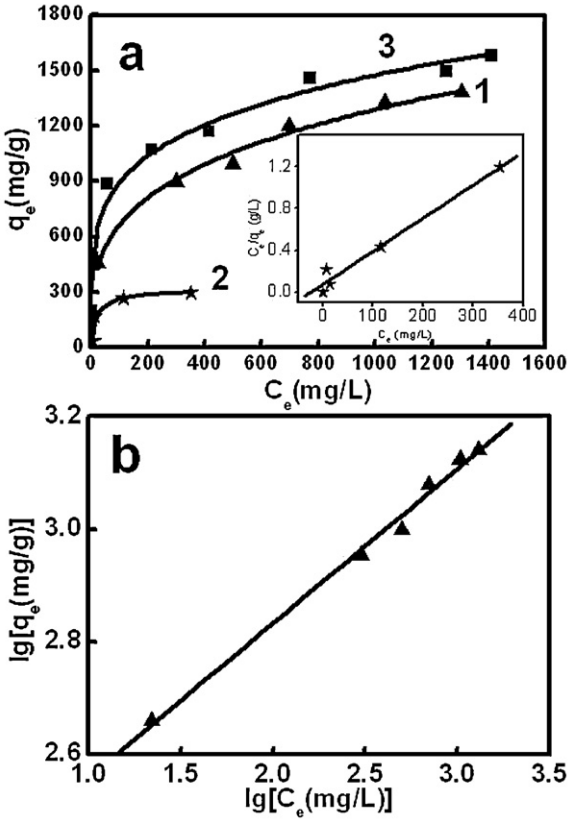

Fig. 3. The adsorption performance of Cu(II) ions on the different absorbents. (a) The adsorption isotherms on the ZnO hollow microspheres with exposed porous nanosheets surface (curve 1) [23], the commercial ZnO powders (curve 2) and the pure porous ZnO nanoplates (curve 3) [22]. The inset is the plot of $C_e/q_e \sim C_e$ corresponding to curve 2) [22]. (b) The polts of $\lg q_e \sim \lg C_e$ corresponding to curve 1 in (a).

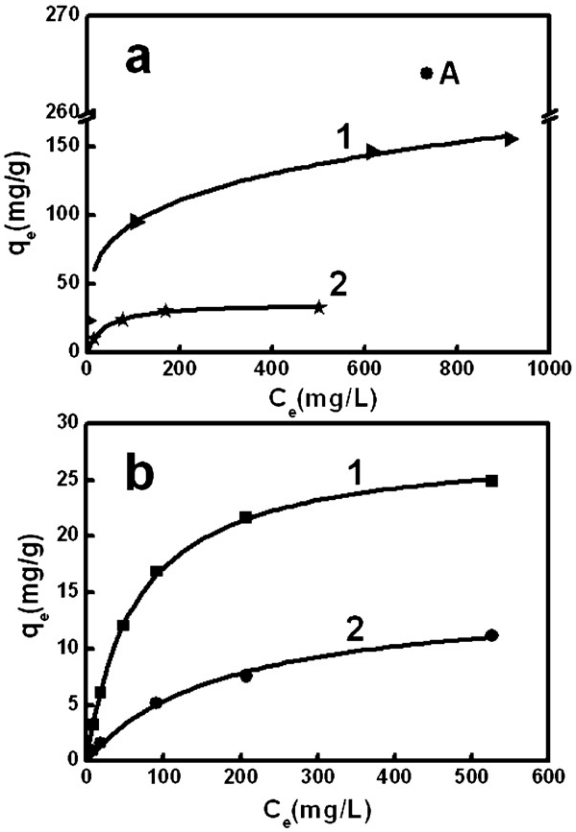

Fig. 4. The adsorption isotherms of Pb(II) ions (a) and Cd(II) ions (b). Curves 1 and 2 correspond to the adsorption on the ZnO hollow microspheres with exposed porous nanosheets surface and the commercial ZnO powders, respectively. Point A in (a) corresponds to the result of Ni(II) adsorption on the ZnO hollow microspheres with exposed porous nanosheets surface [25 °C, pH 6.0].

3.5 respectively, which are close to those of the pure ZnO porous nanoplates with much higher specific surface area [22]. Therefore, the hollow microspheres with exposed porous nanosheets surface is superior to the porous nanoplates in the adsorption efficiency, since the latter is inevitably overlapped during the use and decrease the exposed active surface area.

3.2.2. Extension to adsorption of Pb(II) and Cd(II) ions

Further, we can extend to the other metal ions. Here Pb(II) and Cd(II) were taken as typical heavy metal ions (or adsorbates), which are very toxic pollutants in wastewater and difficult to be removed, to demonstrate the structurally enhanced adsorptive performance of the ZnO hollow microspheres with exposed porous nanosheets surface. Fig. 4 presents their isothermal adsorption curves on the adsorbents (the porous ZnO hollow spheres and commercial ZnO nanopowders). The adsorption amounts increase with increase of concentrations of adsorbates for all samples. The adsorption capacities of the porous ZnO hollow spheres are much higher than that of the commercial ZnO nanopowders and also larger than those of the reported carbon adsorbent [10.86 mg/g for adsorption of Cd(II), 97.08 mg/g for adsorption of Pb(II) ions] [28]. The adsorption behavior of both heavy metal ions followed Langmuir model on the commercial ZnO nanopowders. The order of adsorption capacity to these three metal ions is Cu(II) > Pb(II) > Cd(II), as listed in Table S1.

Similarly, for Pb(II) ions, the adsorption behavior on the porous ZnO hollow spheres is also subject to Freundlich isotherm or Eq. (1), as shown in Fig. 5a. It indicates the unsaturated adsorption. The parameters $K_F = 32.2\,(\mathrm{mg}^{1-1/n}\,\mathrm{L}^{1/n}\,\mathrm{g}^{-1})$ and $n = 4.3$.

For adsorption of Cd(II) ions on the porous ZnO hollow spheres, however, there exists a saturated value, or it follows Langmuir model [32], which describes adsorption on homogeneous surface, namely

$$q_e = \frac{q^0 K_L C_e}{1 + K_L C_e} \quad (2)$$

where q^0 (mg/g) is the saturated adsorption amount, K_L (L/mg) is the constant depicting the affinity in the process of adsorption. The corresponding plot of $C_e/q_e \sim C_e$ is shown in curve 1 of Fig. 5b. The q^0 and K_L values are thus estimated to be 28.1 (mg/g) and 0.02 (L/mg). For the commercial ZnO nanopowders, the adsorptions of all three adsorbates are subject to Eq. (2), or monolayer adsorption, as shown in curves 1′ and 2 of Fig. 5b, and the inset of Fig. 3a. The corresponding parameter values are listed in Table.S1. We can see that the adsorption capacities of Cu(II) and Pb(II) are about 5 times higher on the honeycomb-like porous ZnO hollow spheres than those on the commercial ZnO nanopowders, exhibiting significantly structurally enhanced adsorption performance, while it is only about two times for Cd(II) ion's adsorption.

3.3. Structurally enhanced adsorption and its electronegativity dependence

The strong adsorption performance of the ZnO hollow microspheres with exposed porous nanosheets surface should be related to their unique structure. Such material consists of vertically standing and cross-linked porous nanosheets, which is stable against aggregation, and hence keeps the surface area within the

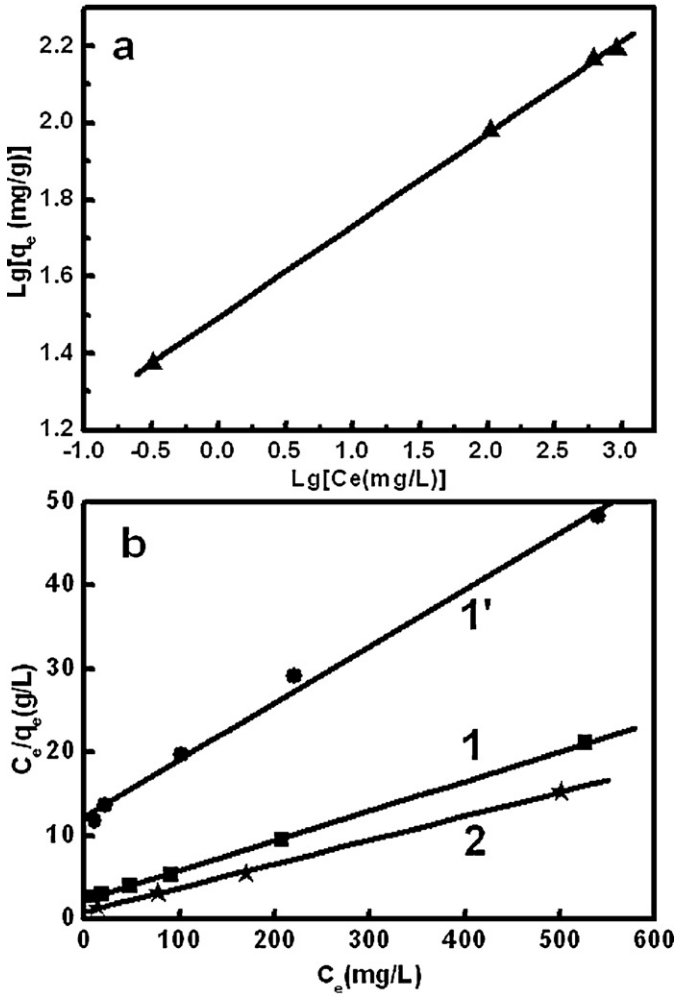

Fig. 5. (a) The plot of lg q_e vs lg C_e for adsorption of Pb(II) ions on the ZnO hollow microspheres with exposed porous nanosheets surface (Freundlich model). (b) : The plots of C_e/q_e vs C_e (Langmiur model). Lines 1 and 1′ are for adsorption of Cd(II) ions on the porous ZnO hollow spheres and the commercial ZnO powders, respectively. Line 2 is for adsorption of Pb (II) ions on the commercial ZnO powders. [data from Fig. 4].

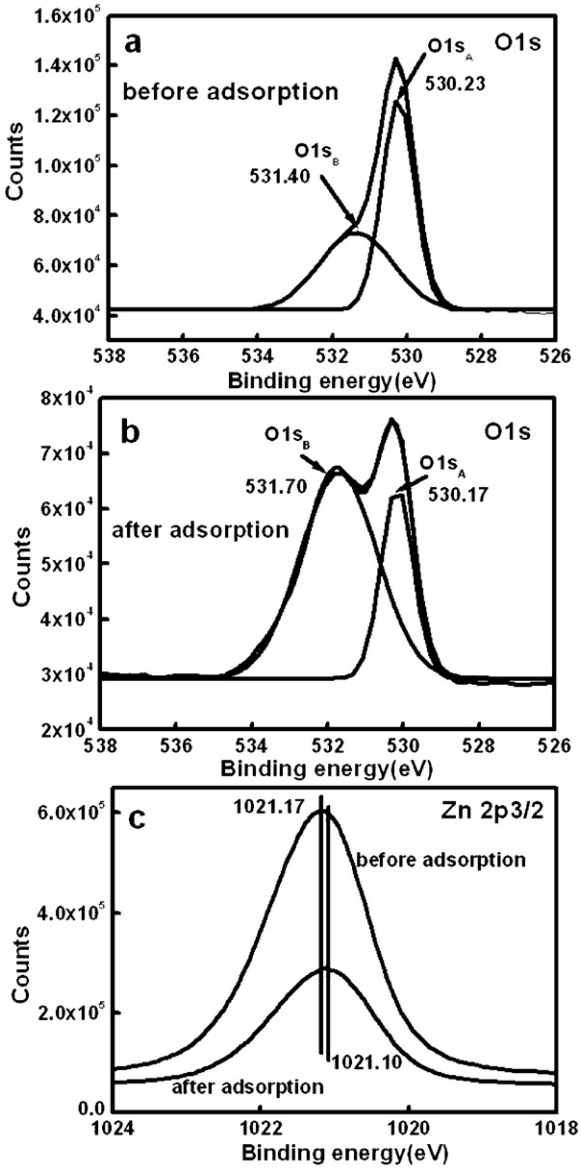

Fig. 6. XPS spectra of O1s (a) and (b) and Zn2p3/2 (c) for the porous ZnO hollow spheres before and after adsorption of Cd(II) ions.

porous nanoplates being sufficiently exposed to the solution. The structurally enhanced adsorption performance would thus be sufficiently exhibited, showing much higher adsorption capacity to the Cu(II), Pb(II) or Cd(II) ions than those on the commercial ZnO powders and the reported carbon adsorbents.

It is well known that hydroxyl groups can be formed on the surface of ZnO during exposure to ambient air or in the water, resulting in negatively charged surface [21]. Existence of the hydroxyl groups in our samples has been confirmed by DRIFT measurement (Fig. S1A). As observed from curve a of Fig. S1A, the peaks at 3687 cm^{-1} and 3616 cm^{-1} can be attributed to the hydroxyl groups formed on the non-polar $(1\,0\,\bar{1}\,0)$ ZnO surface and polar surfaces in the porous structure, respectively [33]. Comparatively, the intensity of former peak is higher than the later, indicates that hydroxyl groups are mainly formed on the exposed non-polar $(1\,0\,\bar{1}\,0)$ surface of ZnO nanosheets. The peak at 3556 cm^{-1} corresponds to hydroxyl groups derived from defects of ZnO hollow spheres. These hydroxyl groups would be actively adsorptive sites [34], and interact with Cu(II), Pb(II) or Cd(II) species to form bonding of Cu—O, Pb—O or Cd—O by Lewis interaction [35], which has been confirmed by the XPS spectral and DRIFT measurements. Typically, Fig. 6 shows the binding energy (BE) spectra of O1s and Zn2p3/2 for the honeycomb-like porous ZnO hollow spheres before and after adsorption of Cd(II) ions. Before adsorption, the spectrum of honeycomb-like porous ZnO hollow spheres consists of $O1s_A$ (530.23 eV) and $O1s_B$ (531.40 eV), which can be ascribed to zinc oxide [36] and hydroxide [37], respectively (Fig. 6a). After adsorption of Cd species, the $O1s_B$ at 531.7 eV is close to that in $Cd(OH)_2$ (530.9 eV) [38], indicating that the Zn—O—H is replaced by Zn—O—Cd, or formation of Cd—O weak bonding, as shown in Fig. 6b. Correspondingly, the BE value of Zn2p3/2 also shifts slightly after adsorption, due to change of the chemical environment for the surface zinc atoms (see Fig. 6c). Similarly, the interaction between hydroxyl groups and heavy metal ions is also demonstrated by DRIFTS, as shown in Fig. S1. After adsorption of heavy metal Cu(II) ions, the peaks at 3453 cm^{-1} and 3340 cm^{-1} are observed which might be ascribed to signals of hydroxyl groups in the Cu—O—H bonding on the non-polar and polar surfaces [39], in addition to the peaks at 3687 cm^{-1} and 3616 cm^{-1} (see curve b of Fig. S1A). Further, the peak at 927 cm^{-1} emerged on curve b of Fig. S1B after adsorption of Cu(II) ions indicates the forming of Cu—O bonding [40].

Although the planar surface of the exposed and cross-linked ZnO nanosheets in the porous ZnO hollow spheres is the non-polar

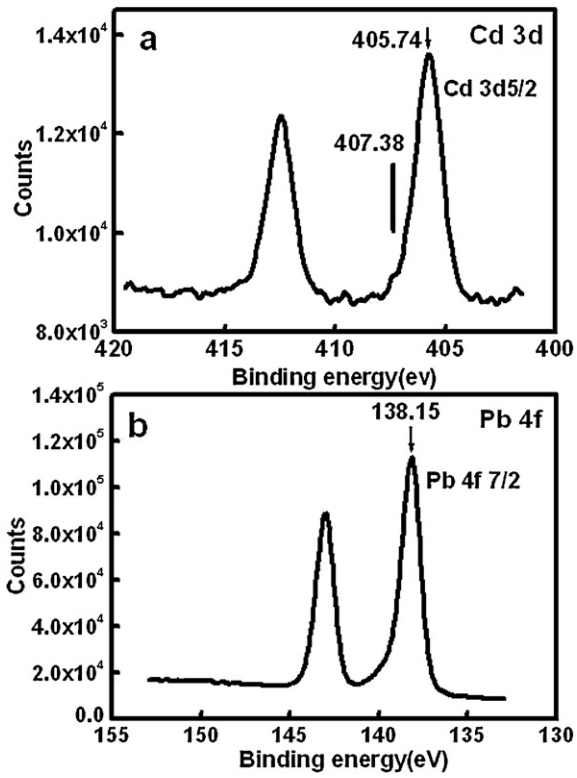

Fig. 7. XPS spectra of Cd3d (a) and Pb4f (b) for the porous ZnO hollow spheres after adsorption of Cd(II) and Pb(II) ions, respectively. Vertical line indicates the position of Cd3d5/2 in CdO.

(1 0 $\bar{1}$ 0)plane, there should exist a large number of polar sites on the wall of pores within the plates due to the porous geometry. It is such the porous geometry that there exist different actively adsorption sites, as demonstrated by DRIFTS (curve a of Fig. S1A), which should correspond to different adsorptive energy levels. Generally, the interaction between the surface of ZnO (or the hydroxyl groups) and the heavy metal ions are closely related to the electronegativity of heavy metal ions [41]. The high electronegativity values would induce the strong interaction which, in turn, corresponds to the more adsorption sites with different adsorptive energy levels and even multi-layer adsorption, showing Freundlich adsorption type. On the contrary, the low electronegativity values will lead to less adsorptive sites due to the weak interaction, exhibiting monolayer adsorption (or Langmuir model). Table S2 gives the electronegativity values for some heavy metal ions. In our case, the electronegativity value is high for Cu(II) (2.00) [42] and Pb(II) (1.87) [43], and low for Cd(II) (1.69) [44], hence keeping the adsorption capacity order Cu(II) > Pb(II) > Cd(II).

To verify such electronegativity dependence of the adsorptive performance, the extended adsorptive measurements were carried out by choosing Ni(II) as an adsorbate, whose electronegativity (1.91) [42] is between those of Cu(II) and Pb(II). For the 10 mL Ni(II) solution with the initial concentration of 1000 mg/L, after addition of 10 mg porous ZnO hollow spheres, the equilibrium adsorptive amount is 264.1 mg/g [see Point A in Fig. 4a]. The adsorption amount of Ni(II) is also between those of Pb(II) and Cu(II).

Also, for Cd(II) ions, they could be mainly adsorbed on the homogeneous exposed non-polar surface due to their low electronegativity value, leading to Langmuir type. However, for adsorption of Cu(II) and Pb(II) ions with larger electronegativity values, they can be adsorbed on the polar sites on the pore walls within the plates in addition to the exposed non-polar planar surface. The adsorption type can be ascribed to Freundlich model owing to their heterogeneous surface adsorption, as demonstrated in Fig. 3b and Fig. 5.

Further, the XPS spectral measurements were performed to examine the electronegativity dependence. Fig. 7 shows the results after Cd(II) and Pb(II) adsorption on the porous ZnO hollow spheres. The BE value of Cd3d5/2 is 405.74 eV, which is much lower than that of CdO (407.38 eV) [45] (Fig. 7a). It means that the adsorbed Cd species are weakly connected with hydroxyl groups on the surface of ZnO, only forming Cd—O weak binding. For Pb(II) adsorption, however, the BE value of Pb4f 7/2 is 138.15 eV, which is very close to that of PbO (138.20 eV) [44] (Fig. 7b), indicating that Pb(II) strongly interact with the surface of ZnO through hydroxyl groups, forming Pb—O bonding.

As for adsorption on the commercial ZnO powders with Langmuir type, it could be attributed to the homogeneous polyhedral surfaces of the ZnO particles (see Fig. S2), which agrees well with the result of our previous work [22].

4. Conclusion

In summary, we have demonstrated that ZnO hollow microspheres with exposed porous nanosheets surface are of significantly structurally enhanced adsorption to the heavy metal cations compared with the commercial ZnO nanopowders due to their unique micro/nanostructure. The adsorption behaviour can be described by Langmuir model, or Freundlich model, depending on the electronegativity of the heavy metals. For the heavy metal with high electronegativity, it can adsorb on the active sites with different adsorptive energy levels due to the large interaction with the adsorbent, showing Freundlich model. Otherwise, the metal with low electronegativity only exhibits Langmuir-type adsorption. Such ZnO hollow microspheres with exposed porous nanosheets surface can be used as efficient adsorbent for removal of heavy metal ions from contaminated water, and easily separated from solution. However, it should be pointed out that the ZnO as an adsorbent should be used in a neutral or weak acid (or alkali) environment because it is unstable in strong acid (or alkali) solutions.

Acknowledgments

This work was financially supported by the National Natural Science Foundation of China(Grant No. 21001002), the China Postdoctoral Science Foundation (No.2011M501407) and the National Basic Research Program of China (Grant No. 2013CB934302).

Appendix A. Supplementary data

Supplementary data associated with this article can be found, in the online version, at http://dx.doi.org/10.1016/j.colsurfa.2013.01.031.

References

[1] X.B. Wang, J. Liu, W.Z. Xu, One-step hydrothermal preparation of amino-functionalized carbon spheres at low temperature and their enhanced adsorption performance towards Cr(VI) for water purification, Colloids Surf. A 415 (2012) 288–294.
[2] R.P. Schwarzenbach, B.I. Escher, K. Fenner, T.B. Hofstetter, C.A. Johnson, U. Gunten, B. Wehrli, The challenge of micropollutants in aquatic systems, Science 313 (2006) 1072–1077.
[3] C. Wang, S.Y. Tao, W. Wei, C.G. Meng, F.Y. Liu, M. Han, Multifunctional mesoporous materials for detection, adsorption and removal of Hg^{2+} in aqueous solution, J. Mater. Chem. 20 (2010) 4635–4641.
[4] J. Theron, J.A. Walker, T.E. Cloete, Nanotechnology and water treatment: applications and emerging opportunities, Crit. Rev. Microbiol. 34 (2008) 43–69.
[5] M. Hua, S.J. Zhang, B.C. Pan, W.M. Zhang, L. Lv, Q.X. Zhang, Heavy metal removal from water/wastewater by nanosized metal oxides: a review, J. Hazard. Mater. 211–212 (2012) 317–331.

[6] F.L. Fu, Q. Wang, Removal of heavy metal ions from wastewaters: a review, J. Environ. Manage. 92 (2011) 407–418.
[7] J.S. Hu, L.S. Zhong, W.G. Song, L.J. Wan, Synthesis of hierarchically structured metal oxides and their application in heavy metal ion removal, Adv. Mater. 20 (2008) 2977–2982.
[8] Y.H. Wang, S.H. Lin, R.S. Juang, Removal of heavy metal ions from aqueous solutions using various low-cost adsorbents, J. Hazard. Mater. 102 (2003) 291–302.
[9] Y. Zhao, L. Jiang, Hollow micro/nanomaterials with multilevel interior structures, Adv. Mater. 21 (2009) 3621–3638.
[10] H. Li, W. Li, Y.J. Zhang, T.S. Wang, B. Wang, W. Xu, L. Jiang, W.G. Song, C.Y. Shu, C.R. Wang, Chrysanthemum-like α-FeOOH microspheres produced by a simple green method and their outstanding ability in heavy metal ion removal, J. Mater. Chem. 21 (2011) 7878–7881.
[11] L.S. Zhong, J.S. Hu, A.M. Cao, Q. Liu, W.G. Song, L.J. Wan, 3D flowerlike ceria micro/nanocomposite structure and its application for water treatment and CO removal, Chem. Mater. 19 (2007) 1648–1655.
[12] H.Y. Xiao, Z.H. Ai, L.Z. Zhang, Nonaqueous sol–gel synthesized hierarchical CeO_2 nanocrystal microspheres as novel adsorbents for wastewater treatment, J. Phys. Chem. C 113 (2009) 16625–16630.
[13] H.X. Zhong, Y.L. Ma, X.F. Cao, X.T. Chen, Z.L. Xue, Preparation and characterization of flowerlike $Y_2(OH)_5NO_3{\cdot}1.5H_2O$ and Y_2O_3 and their efficient removal of Cr(VI) from aqueous solution, J. Phys. Chem. C 113 (2009) 3461–3466.
[14] X.B. Wang, J. Liu, W.Z. Xu, T. Cao, X.J. Song, C.L. Cheng, Preparation of carbon microstructures by thermal treatment of thermosetting/thermoplastic polymers and their application in water purification, Micro Nano Lett. 7 (2012) 918–922.
[15] F. Lu, W.P. Cai, Y.G. Zhang, ZnO hierarchical micro/nanoarchitectures: solvothermal synthesis and structurally enhanced photocatalytic performance, Adv. Funct. Mater. 18 (2008) 1047–1056.
[16] H.B. Zeng, W.P. Cai, P.S. Liu, X.X. Xu, H.J. Zhou, C. Klingshirn, H. Kalt, ZnO-based hollow nanoparticles by selective etching: elimination and reconstruction of metal-semiconductor interface, improvement of blue emission and photocatalysis, ACS Nano 2 (2008) 1661–1670.
[17] N. Han, P. Hu, A. Zuo, D.W. Zhang, Y.J. Tian, Y.F. Chen, Photoluminescence investigation on the gas sensing property of ZnO nanorods prepared by plasma-enhanced CVD method, Sens. Actuators B 145 (2010) 114–119.
[18] Q.F. Zhang, C.S. Dandeneau, S. Candelaria, D.W. Liu, B.B. Garcia, X.Y. Zhou, Y.H. Jeong, G.Z. Cao, Effects of lithium ions on dye-sensitized ZnO aggregate solar cells, Chem. Mater. 22 (2010) 2427–2433.
[19] Z.L. Wang, ZnO nanowire and nanobelt platform for nanotechnology, Mater. Sci. Eng. B 64 (2009) 33–71.
[20] B. Meyer, H. Rabaab, D. Marx, Water adsorption on ZnO(1 0 0): from single molecules to partially dissociated monolayers, Phys. Chem. Chem. Phys. 8 (2006) 1513–1520.
[21] Y. Kikuchi, Q.R. Qian, M. Machida, H. Tatsumoto, Effect of ZnO loading to activated carbon on Pb(II) adsorption from aqueous solution, Carbon 44 (2006) 195–202.
[22] X.B. Wang, W.P. Cai, Y.X. Lin, G.Z. Wang, C.H. Liang, Mass production of micro/nanostructured porous ZnO plates and their strong structurally enhanced and selective adsorption performance for environmental remediation, J. Mater. Chem. 20 (2010) 8582–8590.
[23] X.B. Wang, W.P. Cai, G.Z. Wang, C.H. Liang, Standing porous ZnO nanoplate-built hollow microspheres and kinetically controlled dissolution/crystal growth mechanism, J. Mater. Res. 27 (2012) 951–958.
[24] Z.H. Jing, J.H. Zhan, Fabrication and gas-sensing properties of porous ZnO nanoplates, Adv. Mater. 20 (2008) 4547–4551.
[25] X.Y. Zeng, J.L. Yuan, L.D. Zhang, Synthesis and photoluminescent properties of rare earth doped ZnO hierarchical microspheres, J. Phys. Chem. C 112 (2008) 3503–3508.
[26] S. Brunauer, L.S. Deming, W.E. Deming, E. Teller, On a theory of the van der Waals adsorption of gases, J. Am. Chem. Soc. 62 (1940) 1723–1732.
[27] S. Brunauer, P.H. Emmett, E. Teller, Adsorption of gases in multimolecular layers, J. Am. Chem. Soc. 60 (1938) 309–319.
[28] Y.H. Li, J. Dinga, Z. Luanb, Z. Dia, Y. Zhua, C. Xua, D. Wu, B. Wei, Competitive adsorption of Pb^{2+}, Cu^{2+} and Cd^{2+} ions from aqueous solutions by multiwalled carbon nanotubes, Carbon 41 (2003) 2787–2792.
[29] K. Kadirvelu, J. Goel, C. Rajagopal, Sorption of lead, mercury and cadmium ions in multi-component system using carbon aerogel as adsorbent, J. Hazard. Mater. 153 (2008) 502–507.
[30] W. Yantasee, Y.H. Lin, G.E. Fryxell, K.L. Alford, B.J. Busche, C.D. Johnson, Selective removal of copper(II) from aqueous solutions using fine-grained activated carbon functionalized with amine, Ind. Eng. Chem. Res. 43 (2004) 2759–2764.
[31] H. Freundlich, W. Heller, Rubber die adsorption in lusungen, J. Am. Chem. Soc. 61 (1939) 2228–2230.
[32] I. Langmuir, The adsorption of gase on plane surfaces of glass, mica and platinum, J. Am. Chem. Soc. 40 (1918) 1361–1403.
[33] H. Hoei, H.S. Qiu, Y.M. Wang, E. Löffler, C. Wöll, M. Muhler, The identification of hydroxyl groups on ZnO nanoparticles by infrared spectroscopy, Phys. Chem. Chem. Phys. 10 (2008) 7092–7097.
[34] Y.J. Xu, G. Weinberg, X. Liu, O. Timpe, R. Schlögl, D.S. Su, Nanoarchitecturing of activated carbon: new facile strategy for chemical functionalization of the surface of activated carbon, Adv. Funct. Mater. 18 (2008) 3613–3619.
[35] G. Ballerini, K. Ogle, M.G. Barthés-Labrousse, The acid–base properties of the surface of native zinc oxide layers: an XPS study of adsorption of 1,2-diaminoethane, Appl. Surf. Sci. 253 (2007) 6860–6867.
[36] V.I. Nefedov, M.N. Firsov, I.S. Shaplygin, Electronic-structures of $MRhO_2$, MRh_2O_4, $RhMO_4$ and Rh_2MO_6 on the basis of X-ray spectroscopy and ESCA data, J. Electron Spectrosc. Relat. Phenom. 26 (1982) 65–78.
[37] J.S. Mrowiecka, S. Zanna, K. Ogle, P. Marcus, Adsorption of 1,2-diaminoethane on ZnO thin films from p-xylene, Appl. Surf. Sci. 254 (2008) 5530–5539.
[38] J.S. Hammond, S.W. Gaarenstroom, N. Winograd, X-ray photoelectron spectroscopic studies of cadmium- and silver–oxygen surfaces, Anal. Chem. 47 (1975) 2193–2199.
[39] J. Valyont, W.K. Hall, Effects of reduction and reoxidation on the infrared spectra from Cu-Y and Cu-ZSM-5 zeolites, J. Phys. Chem. 97 (1993) 7054–7060.
[40] J. Valyon, W.K. Hall, Studies of the desorption of oxygen from Cu-zeolites during NO decomposition, J. Catal. 143 (1993) 520–532.
[41] R.D. Cakan, N. Baccile, M. Antonietti, M.M. Titirici, Carboxylate-rich carbonaceous materials via one-step hydrothermal carbonization of glucose in the presence of acrylic acid, Chem. Mater. 21 (2009) 484–490.
[42] C.F. Brasquet, Z. Reddad, K. Kadirvelu, P.L. Cloirec, Modeling the adsorption of metal ions (Cu^{2+}, Ni^{2+}, Pb^{2+}) onto ACCs using surface complexation models, Appl. Surf. Sci. 196 (2002) 356–365.
[43] H. Benhima, M. Chiban, F. Sinan, P. Seta, M. Persin, Removal of lead and cadmium ions from aqueous solution by adsorption onto micro-particles of dry plants, Colloids Surf. B 61 (2008) 10–16.
[44] W.E. Morgan, J.R. Vanwazer, Binding-energy shifts in the X-ray photoelectron spectra of a series of related group IVa compounds, J. Phys. Chem. 77 (1973) 964–969.
[45] M.S. Setty, A.P.B. Sinha, Characterization of highly conduction PbO-doped Cd_2SnO_4 thick films, Thin Solid Films 144 (1986) 7–19.